

Analysis of Microwave Absorption Caused by Free Carriers in Silicon

Toshiyuki Sameshima, Hiromi Hayasaka, and Tomonori Haba

Tokyo University of Agriculture and Technology, 2-24-16 Naka-cho, Koganei, Tokyo 184-8588, Japan

Received August 2, 2008; accepted October 18, 2008; published online February 20, 2009

Microwave absorption caused by free carriers was investigated. A 9.35 GHz microwave interferometer was constructed. The transmissivity of 525- μm -thick silicon substrates decreased from 60.4 to 3.8% as the resistivity decreased from 1000 to 4 $\Omega\text{ cm}$. This characteristic was explained well by a numerical analysis using the free carriers absorption theory. Microwave free carrier photo absorption caused by light-induced carriers was also investigated for p-type silicon samples coated with 100 nm thermally grown SiO_2 layers as well as SiO_x layers deposited by the vacuum evaporation method. The effective minority carrier lifetime and recombination velocity were analyzed in the case of the photo induced carrier generation with 532 nm light illumination. The effective minority carrier lifetime was increased from 360 to 540 μs and the recombination velocity was decreased from 78 to 30 cm/s by 1.3×10^6 Pa H_2O vapor heat treatment at 260 $^\circ\text{C}$ for 3 h for light illumination at 0.315 mW/cm^2 in the case of the thermally grown SiO_2/Si because of the passivation of SiO_2/Si interfaces. They were markedly increased from 30 to 380 μs and from 1300 to 60 cm/s, respectively, by the H_2O vapor heat treatment in the case of the vacuum-evaporated SiO_x/Si . © 2009 The Japan Society of Applied Physics

DOI: 10.1143/JJAP.48.021204

1. Introduction

The nondestructive and noncontact measurement of the electrical properties of a semiconductor is attractive for the monitoring of samples during device fabrication. Free carrier optical absorption effect is sensitive in the microwave region. Free carriers in semiconductors respond to the incident electrical field of microwave on the order of GHz, and complex refractive indexes can be changed so that the transmissivity changes with the density of free carriers. The carrier density and its spatial distribution depend on the bulk and interface properties. Carriers can be trapped or recombined at the SiO_2/Si interfaces when there are many defect states.¹⁾ Analysis of photo induced carrier properties is also important for photovoltaic devices such as solar cells. Measurements of microwave photoconductive decay^{2,3)} and quasi-steady-state photoconductance (QSSPC)⁴⁾ have been widely used for the measurement of the photo induced minority carrier lifetime.

In this paper, we report a precise measurement method of determining the carrier density in silicon using the microwave free carrier absorption effect. We present a microwave interferometer developed for sensitive detection of free carrier absorption. We discuss our theory for estimating the carrier density. We demonstrate free carrier absorption effects induced by carriers in silicon substrates with different doping concentrations. The density of the photo induced carrier in silicon caused by light illumination is also reported. We also report changes in the photo induced carrier density, effective minority carrier lifetime and recombination velocity induced by surface passivation by high-pressure H_2O vapor heat treatment.

2. Experimental Procedure

Figure 1(a) shows a schematic of the free carrier absorption measurement system. The 9.35 GHz microwave was emitted by a field-effect-transistor (FET)-type oscillator. Its intensity was modulated at a frequency of 1 kHz. The microwave was introduced using a waveguide tube. It was symmetrically split into two branches by a T-type waveguide. There was a 1 mm gap in each branch for the measurement of sample wafers, which were inserted in gaps A and B, respectively. The microwaves transmitted through the samples were

combined using another T-type waveguide, as shown in Fig. 1(a). The intensities of the sum I_{A+B} and difference I_{A-B} of the microwaves in the two branches were detected by high-speed diode rectifiers, and the signals were amplified by 1-kHz-lock-in amplifiers. The intensities I_{A+B} and I_{A-B} are expressed as

$$I_{A+B} = a|E_A + E_B|^2, \quad (1)$$

$$I_{A-B} = a|E_A - E_B|^2, \quad (2)$$

where E_A and E_B are the electrical field amplitudes transmitted through sample A and B, respectively, and a is a proportionality factor. If the measurement system had an ideal symmetric structure, and there were no samples in the two gaps, the intensities I_{A+B} and I_{A-B} are expressed as

$$I_{A+B} = I_0 = 4a|E_{B0}|^2, \quad (3)$$

$$I_{A-B} = 0, \quad (4)$$

where E_{B0} is the initial electrical field amplitudes for each branch.

When a sample is inserted at gap A, while gap B is kept blank, the intensity I_{A+B} and I_{A-B} are expressed as

$$I_{A+B} + I_{A-B} = 2a(|E_A|^2 + |E_{B0}|^2). \quad (5)$$

The transmissivity of the sample A is obtained as

$$T_A = \frac{|E_A|^2}{|E_{B0}|^2} = 2 \frac{I_{A+B} + I_{A-B}}{I_0} - 1. \quad (6)$$

If the transmissivity of a reference material is already given, the present system precisely gives a difference in transmissivity between a sample and a reference as

$$T_A = T_B \left(2 \frac{I_{A+B} + I_{A-B}}{I_B} - 1 \right), \quad (7)$$

where I_B is the intensity of the sum of the two microwaves when two reference samples with the same type were inserted in the two gaps. The detection accuracy of the present system in the transmissivity was $\pm 0.1\%$.

Silicon wafers with a thickness of 525 μm and different resistivities from 4 to 1000 $\Omega\text{ cm}$ were prepared in order to demonstrate the measurement of the transmissivity at 9.35 GHz using the present system and the effect of free carrier absorption on the transmissivity. The silicon wafer was inserted to gap A, while gap B was blank.

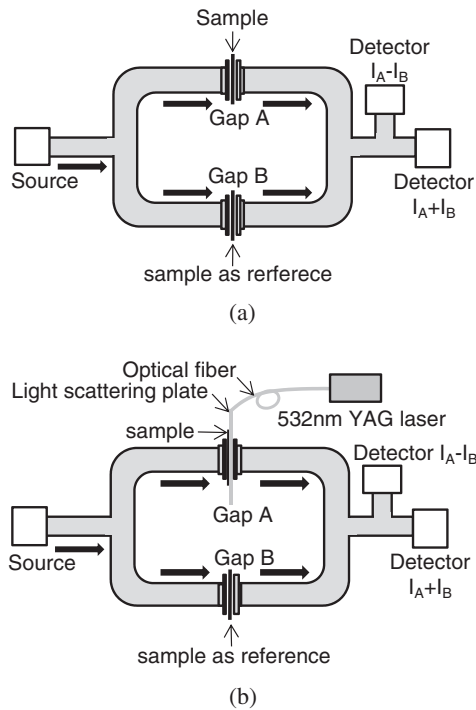


Fig. 1. Schematic of the free carrier absorption measurement system (a) and photo induced carrier generation measurement system (b).

Photo induced carriers generated in silicon wafers were also investigated. A thin light-scattering plate was inserted into gap A facing the samples as shown in Fig. 1(b). A laser light at 532 nm was introduced using optical fibers to the light-scattering plate, which gave uniform green illumination to the samples. The intensity of the laser light was controlled from 0 to 3.27 mW/cm² at the sample surface. The four types of silicon wafer were fabricated using p-type silicon wafers with resistivity ranging 22–23.5 Ω cm (carrier concentration ranging from 6.0 × 10¹⁴–5.5 × 10¹⁴ cm⁻³) and a thickness of 625 μm. The surfaces of every silicon wafer were coated with 100 nm thick SiO₂ layers by the thermally grown method at 1100 °C at first. The silicon wafer coated with thermally grown SiO₂ layers was used at gap B as reference. A similar silicon wafer coated with thermally grown SiO₂ layers was also inserted in gap A and illuminated with a 532 nm green laser light for photo induced carrier measurement (sample 1). Heat treatment in 1.3 × 10⁶ Pa H₂O vapor at 260 °C for 3 h was also applied to the sample measured at gap A to reduce the density of defect states localized at the SiO₂/Si interface (sample 2).⁵⁾ In order to investigate the low-temperature passivation of the silicon surface, SiO_x films were deposited at room temperature on the top silicon surface by the vacuum evaporation of powdered SiO at a base pressure of 4 × 10⁻⁴ Pa after removing the thermally grown SiO₂ layer using buffered HF solution at the top surface and keeping the thermally grown SiO₂ at the rear surface (sample 3). Heat treatment in 1.3 × 10⁶ Pa H₂O vapor at 260 °C for 3 h was also applied to the sample to reduce the density of defect states localized at the SiO_x/Si interface (sample 4). The optical reflectivity at 532 nm was measured on the surface of samples coated with thermally grown SiO₂ as well as vacuum-evaporated SiO_x films.

3. Theory and Analysis

We analyzed the free carrier absorption effect in silicon at 9.35 GHz microwave. The free carrier absorption effect is explained using the Drude theory.^{6,7)} Free carriers in silicon vibrate according to the electrical field of the microwave. The vibration of free carriers causes polarization, which induces change in the effective dielectric constant. The real part ε_r and ε_i of the complex dielectric constant of silicon are expressed as

$$\epsilon_r = n_f^2 - k_f^2 = \epsilon_{Si} \left(1 - \frac{\omega_p^2 \tau^2}{1 + \omega^2 \tau^2} \right), \quad (8)$$

$$\epsilon_i = 2n_f k_f = \epsilon_{Si} \frac{\omega_p^2 \tau}{\omega(1 + \omega^2 \tau^2)}, \quad (9)$$

where ω is the angular frequency, ε_{Si} is the dielectric constant of intrinsic silicon, n_f is the refractive index of silicon, k_f is the extinction coefficient induced by free carrier optical absorption, τ is the lifetime of carriers, and ω_p is the plasma angular frequency expressed as

$$\omega_p = \sqrt{\frac{Ne^2}{m\epsilon_{Si}}}, \quad (10)$$

where N is the majority carrier density, e is the elemental charge, and m is the effective mass of the carrier. ε_r decreases when free carrier vibration occurs because of the anti-phase vibration. ε_i and k_f increase and absorption of the microwave significantly occurs when many carriers cause polarization by responding to the incident microwave. ε_i and k_f are high when the angular frequency is low. Therefore, the free carrier absorption is sensitively observed at the 9.35 GHz microwave frequency. For crystalline silicon, the resistivity determines the carrier density and carrier mobility, because the relation between the carrier density and carrier mobility has been well defined.⁸⁾ The carrier lifetime is given using the carrier mobility μ as,

$$\tau = \frac{m}{e} \mu. \quad (11)$$

We constructed a calculation program by a finite element method with a lattice distance of 1 μm using the statistically thermodynamical semiconductor band theory⁹⁾ and including free carrier optical absorption given using eqs. (8)–(10) and the optical interference effect¹⁰⁾ using a Fresnel coefficient at each lattice in order to calculate the transmissivity of the sample. The wavelength of the 9.35 GHz microwave is 3.21 cm, which is much longer than the thickness of the silicon wafers. Figure 2 shows the calculated transmissivity as a function of the resistivity of silicon wafers with difference thicknesses. The transmissivity monotonically decreased as the resistivity decreased for each wafer thickness because of serious free carrier absorption effect. It was high when the wafer was very thin because a thin wafer does not change the phase of the electrical field so much, so that the difference in the refractive index between silicon and air is not so important in transmissivity. When the wafer thickness increased, the transmissivity decreased because the free carrier absorption effect became considerable particularly for low-resistivity conditions. In addition, the reflectivity increased as the wafer thickness increased owing to the optical interference effect

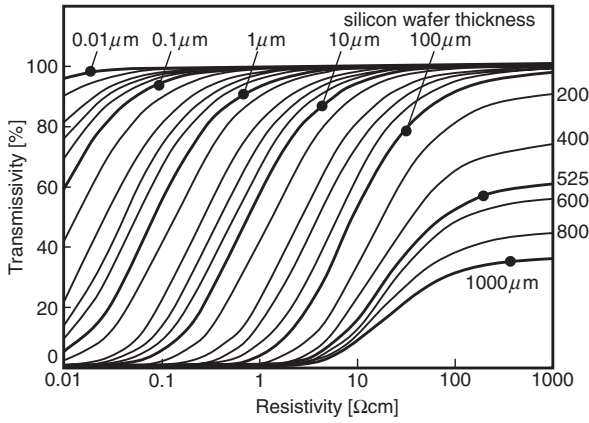


Fig. 2. Calculated transmissivity as a function of the resistivity of silicon wafers with difference thicknesses.

because the phases between microwaves reflected at the top and rear sample surfaces became equal as the wafer thickness increased. For example, the transmissivity decreased in the case of a high resistivity of 1000 Ω cm as the wafer thickness increased because of reflection loss, although the free carrier absorption effect was not important because of the low carrier density.

The effect of photo induced carriers was also analyzed. The density of photo carriers N_{photo} is continuously generated by illumination with green light, the majority carrier density is $N + N_{\text{photo}}$ and the minority carrier density is N_{photo} . The complex dielectric constants are given as

$$\epsilon_r = \epsilon_{\text{Si}} \left(1 - \frac{\omega_{p1}^2 \tau_1^2}{1 + \omega^2 \tau_1^2} - \frac{\omega_{p2}^2 \tau_2^2}{1 + \omega^2 \tau_2^2} \right), \quad (12)$$

$$\epsilon_i = \epsilon_{\text{Si}} \left[\frac{\omega_{p1}^2 \tau_1}{\omega(1 + \omega^2 \tau_1^2)} + \frac{\omega_{p2}^2 \tau_2}{\omega(1 + \omega^2 \tau_2^2)} \right], \quad (13)$$

where τ_1 and τ_2 are the lifetimes of the majority carriers and minority carriers, respectively, which are assumed to be given by the hole and electron carrier mobilities at the substrate doping concentration, and ω_{p1} and ω_{p2} are the

plasma angular frequencies of the majority carriers and minority carriers, respectively.

Light illumination with an intensity of W per unit area gives a photon flux $G = W/h\nu$ per unit area, where h is the plank constant and ν is the frequency of the green laser light. When the density of the photo induced carrier caused by photon flux G is sufficiently lower than the density of the majority carriers per unit area, the photo induced carrier density in-depth distribution $N_{\text{photo}}(x)$ is given using the carrier diffusion model for a steady state condition as¹¹⁾

$$D \frac{d^2 N_{\text{photo}}(x)}{dx^2} - \frac{N_{\text{photo}}(x)}{\tau_b} = 0, \quad (14)$$

where D is the carrier diffusion coefficient and τ_b is the minority bulk carrier lifetime, which is far different from the carrier lifetimes τ_1 and τ_2 previously shown in eqs. (12) and (13). Although τ_1 and τ_2 typically range from 0.07 to 0.2 ps, the minority carrier bulk lifetime is much longer because it is the time constant of carrier annihilation. The present silicon wafers with the carrier concentration ranging from 6.0×10^{14} – $5.5 \times 10^{14} \text{ cm}^{-3}$ typically have an electron minority carrier bulk lifetime of about 1 ms based on a previous study.¹²⁾ Laser light at 532 nm illuminated at the top surface is absorbed within the top 1 μm depth because of the high absorption coefficient of about 10^4 cm^{-1} . We therefore place the boundary condition of carrier generation and carrier recombination ratios as

$$D \frac{dN_{\text{photo}}}{dx} \Big|_{x=0} = S_1 N_{\text{photo}}(0) - \eta(1-r)G, \quad (15)$$

$$D \frac{dN_{\text{photo}}}{dx} \Big|_{x=d} = -S_2 N_{\text{photo}}(d), \quad (16)$$

where S_1 and S_2 are recombination velocities of the two surfaces of silicon, η is the quantum efficiency for photo induced carrier generation, which is assumed as 1 in this investigation, r is the optical reflectivity of the green laser light, d is the thickness of the silicon wafer and the rear surface point. Equations (15) and (16) give the density of photo induced carrier $N_{\text{photo}}(x)$ as

$$N_{\text{photo}}(x) = N_0 \left[\left(\sqrt{\frac{D}{\tau_b}} - S_2 \right) \exp\left(-\frac{x}{\sqrt{D\tau_b}}\right) + \left(\sqrt{\frac{D}{\tau_b}} + S_2 \right) \exp\left(-\frac{2d-x}{\sqrt{D\tau_b}}\right) \right]$$

$$N_0 = \frac{\eta(1-r)G}{\left(\sqrt{\frac{D}{\tau_b}} - S_2 \right) \left(\sqrt{\frac{D}{\tau_b}} + S_1 \right) - \left(\sqrt{\frac{D}{\tau_b}} - S_1 \right) \left(\sqrt{\frac{D}{\tau_b}} + S_2 \right) \exp\left(-\frac{2d}{\sqrt{D\tau_b}}\right)}. \quad (17)$$

The total photo induced minority carrier density per unit area n is obtained by the integration of $N_{\text{photo}}(x)$ from 0 to d as

$$n = N_0 \sqrt{D\tau_b} \left[1 - \exp\left(-\frac{d}{\sqrt{D\tau_b}}\right) \right] \left[\sqrt{\frac{D}{\tau_b}} - S_2 + \left(\sqrt{\frac{D}{\tau_b}} + S_2 \right) \exp\left(-\frac{d}{\sqrt{D\tau_b}}\right) \right]. \quad (18)$$

In the present case, the electron minority carrier diffusion coefficient D is $36 \text{ cm}^2 \text{ V}^{-1} \text{ s}^{-1}$. We also assume that both surfaces coated with thermally grown SiO_2 have the same quality with the same minority carrier recombination velocity.

Our program results in $N_{\text{photo}}(x)$ at each lattice site using input data of η , G , r , d , D , τ_b , S_1 , and S_2 , as shown in eqs. (14)–(18). It subsequently calculates change in the

complex refractive index caused by $N_{\text{photo}}(x)$ as given in eqs. (12) and (13), and then calculates change in transmissivity at 9.35 GHz using the Fersnel optical interference with the change in the complex refractive index in the entire wafer thickness. When G or τ_b increases, $N_{\text{photo}}(x)$ becomes high and the transmissivity markedly decreases because of substantial free carrier absorption. On the other hand, when S_1 or S_2 increases, $N_{\text{photo}}(x)$ does not increase so much and

the transmissivity remains similar to the value in the dark field. The calculation program confirmed that the detection accuracy of 0.1% of the present microwave equipment allowed us to observe change in a photo induced carrier density per unit area of $5 \times 10^{10} \text{ cm}^{-2}$, when silicon wafers had a resistivity of $22 \text{ } \Omega \text{ cm}$ and a thickness of $625 \text{ } \mu\text{m}$. It means that the present measurement and analysis system can be used to investigate the photo induced carrier behavior under a low injection condition. Moreover, our calculated investigation revealed that the transmissivity was governed by the photo induced carrier density per unit area n given in eq. (18), and that it did not depend on the distribution of $N_{\text{photo}}(x)$ in the thickness direction, in the cases of n ranging from 1×10^{10} to $1 \times 10^{14} \text{ cm}^{-2}$ and of S_1 and S_2 ranging from 0 to 2000 S/cm . Carrier injection caused by light illumination at the top surface and recombination velocities of S_1 and S_2 can cause distributions of $N_{\text{photo}}(x)$ as well as the complex refractive index in the thickness direction. Their distributions in the silicon wafer with a thickness of $625 \text{ } \mu\text{m}$ did not affect the transmissivity because the wafer thickness is much smaller than the microwave wavelength. It indicates that the experimentally observed transmissivity directly gives the photo induced minority carrier density per unit area n . Therefore, n gives the effective minority carrier lifetime τ_{eff} as

$$n = \eta(1 - r)G\tau_{\text{eff}}, \quad (19)$$

where carrier annihilation rates at the surfaces as well as in the silicon bulk are reciprocally represented by τ_{eff} , which corresponds to the effective minority carrier lifetime obtained by conventional equipment.²⁻⁴⁾ When τ_b is given, S_1 and S_2 as well as $N_{\text{photo}}(x)$ can be analyzed using eqs. (17) and (18).

4. Results and Discussion

Figure 3 shows the experimental and calculated transmissivities for a thickness of $525 \text{ } \mu\text{m}$ as a function of the resistivity of silicon wafers. The transmissivity decreased from 60.4 to 3.8% as the resistivity decreased from 1000 to $4 \text{ } \Omega \text{ cm}$ because the carrier density increased in silicon substrates and the effect of free carrier photo absorption increased. Good agreement between experimental and calculated transmissivities shows that the present method can be used to precisely analyze the resistivity and conductivity of silicon.

Figure 4 shows the transmissivity (a) and the density of photo induced minority carriers per unit area (b) as a function of the intensity of 532 nm light illumination for four types of silicon samples. Solid triangles show transmissivity for the sample with both surfaces coated with thermally grown SiO_2 layers. Open triangles show transmissivity after high-pressure H_2O vapor annealing of the sample with both surfaces coated with thermally grown SiO_2 layers. Solid circles show transmissivity for the sample with the top surface coated with SiO_x layers. Open circles show transmissivity after high-pressure H_2O vapor annealing of the sample with the top surface coated with SiO_x layers. The transmissivity ranged from 26.5 to 27.6% under the dark-field condition as shown in Fig. 4(a). This probably results from the change in free carrier absorption caused by variation in the hole carrier concentration of silicon wafers

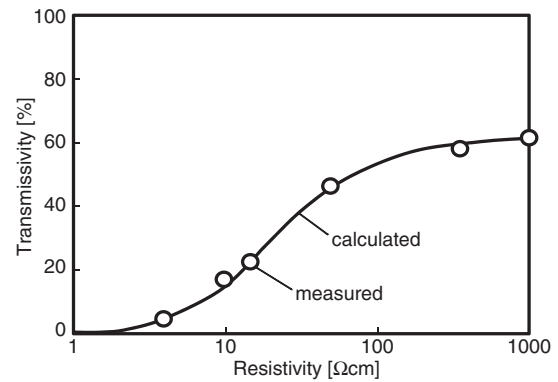


Fig. 3. Experimental and calculated transmissivities and carrier densities for a thickness of $525 \text{ } \mu\text{m}$ as a function of the resistivity of silicon wafers.

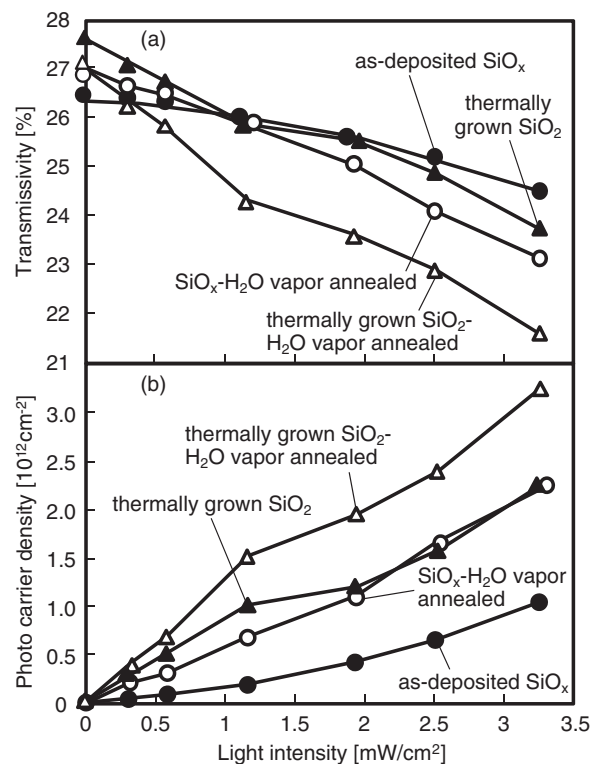


Fig. 4. Transmissivity (a) and density of photo induced minority carriers per unit area (b) as a function of the intensity of 532 nm light illumination for four types of silicon sample coated with thermally grown SiO_2 (solid triangles) and annealed with high-pressure H_2O vapor (open triangles), and as-deposited SiO_x layers on the top surface (solid circles) and annealed with high-pressure H_2O vapor (open circles).

ranging from 5.6×10^{14} to $6.1 \times 10^{14} \text{ cm}^{-3}$. The transmissivity monotonically decreased as the light intensity increased from 0 (dark field) to 3.27 mW/cm^2 for every sample. This is because of the free carrier absorption by photo induced carriers. The sample with both surfaces coated with thermally grown SiO_2 and annealed with high-pressure H_2O vapor showed the highest decrease in transmissivity from 27.1 to 21.6% as the light intensity increased from 0 to 3.27 mW/cm^2 . On the other hand, the sample with the as-deposited SiO_x layer on the top surface showed the lowest decrease in transmissivity from 26.5 to 24.5%. The

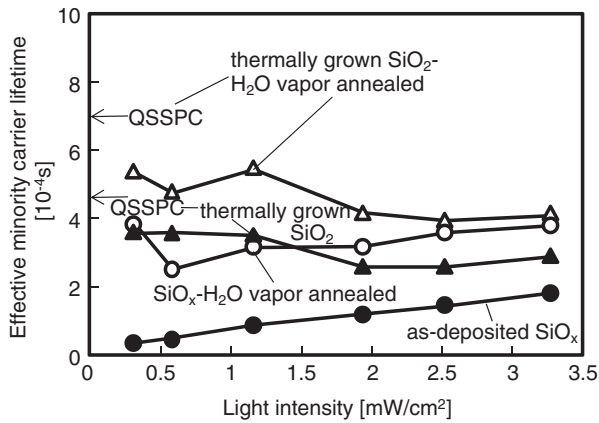


Fig. 5. Effective minority carrier lifetime analyzed from the results of Fig. 4 as a function of the intensity of 532 nm light illumination for the four types of silicon sample. Effective minority carrier lifetime obtained by QSSPC are also presented by arrows for silicon samples coated with thermally grown SiO_2 and high-pressure.

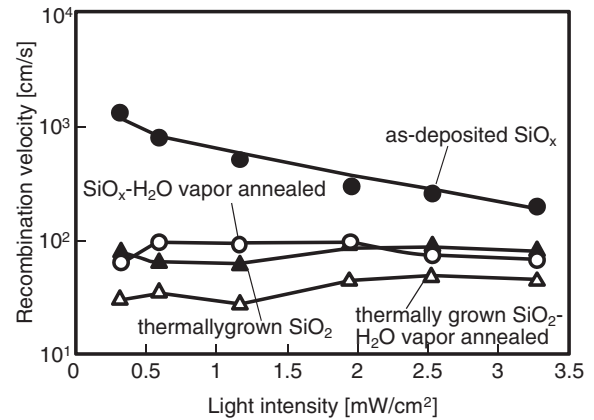


Fig. 6. Recombination velocity analyzed from the results of Fig. 5 as a function of the intensity of 532 nm light illumination for the four types of silicon sample.

density of photo induced minority carriers per unit area was obtained by analysis of the experimental transmissivity, as shown in Fig. 4(a), using the free carrier absorption theory. It increased as the intensity of light illumination increased for every sample. The sample with both surfaces coated with thermally grown SiO_2 and annealed with high-pressure H_2O vapor had the highest density of photo induced carriers of $3.2 \times 10^{12} \text{ cm}^{-2}$ at $3.27 \text{ mW}/\text{cm}^2$. On the other hand, the sample with the as-deposited SiO_x layer on the top surface had the lowest density of photo induced carriers of $1.0 \times 10^{12} \text{ cm}^{-2}$ at $3.27 \text{ mW}/\text{cm}^2$.

Figure 5 shows the effective minority carrier lifetime obtained from the results of Fig. 4 for the four samples. The sample treated by high-pressure H_2O vapor annealing of silicon with both surfaces coated with thermally grown SiO_2 had the highest effective minority carrier lifetimes ranging from 400 to $540 \mu\text{s}$ for the light intensity ranging from 0.315 to $3.27 \text{ mW}/\text{cm}^2$. On the other hand, the sample with both surfaces coated with thermally grown SiO_2 before high-pressure H_2O vapor annealing had an effective minority carrier lifetime ranging from 260 to $360 \mu\text{s}$. High-pressure H_2O vapor heat treatment increased the effective minority carrier lifetime because of the passivation of thermally grown SiO_2/Si interfaces. The sample with the as-deposited SiO_x layer on the top surface had low effective minority carrier lifetimes, which markedly increased from 30 to $180 \mu\text{s}$ as the light intensity increased from 0.315 to $3.27 \text{ mW}/\text{cm}^2$. It indicates that the as-deposited SiO_x/Si interface had substantial defect states that reduced the effective minority carrier lifetime. The effective minority carrier lifetime was increased by high-pressure H_2O vapor annealing to 250 to $380 \mu\text{s}$ similar to that of the sample coated with thermally grown SiO_2 layers. This indicates that high-pressure H_2O vapor heat treatment effectively passivated the SiO_x/Si interfaces. The results of Figs. 4 and 5 show that the present measurement system gives precise information on photo induced carrier behaviors in the case of low carrier injection conditions. The effective minority carrier lifetime was also measured using a conventional QSSPC equipment for the sample with both surfaces coated with thermally grown SiO_2 and that sample treated by high-

pressure H_2O vapor annealing for comparison of the present method. In QSSPC measurements, the effective minority carrier lifetime was obtained from the change in the circuit impedance that was detected during and after Xenon lamp illumination with an intensity of $6.4 \text{ W}/\text{cm}^2$ for 2.3 ms using a 2-cm-diameter coil at a frequency of 13.56 MHz. The effective minority carrier lifetime was $470 \mu\text{s}$ for the sample with both surfaces coated with thermally grown SiO_2 . It was increased to $690 \mu\text{s}$ by high-pressure H_2O vapor annealing. The effective minority carrier lifetime obtained by QSSPC was larger than that obtained by the present method for each sample. The fact that the light intensity for QSSPC was much higher than that for the present condition makes us believe that the present results of the effective minority carrier lifetime are comparable to those obtained by conventional methods.

When the electron minority carrier bulk lifetime was assumed to be 1 ms for the four types of silicon sample, the surface recombination velocity was estimated by analysis of free carrier absorption combined with the carrier diffusion theory given using eqs. (14)–(19), as shown in Fig. 6. The sample treated with high-pressure H_2O vapor annealing of silicon with both surfaces coated with thermally grown SiO_2 had the lowest recombination velocity ranging from 25 to $45 \text{ cm}/\text{s}$, which was almost constant for the light intensity ranging from 0.315 to $3.27 \text{ mW}/\text{cm}^2$. On the other hand, the sample with both surfaces coated with thermally grown SiO_2 had the recombination velocity ranging from 65 to $90 \text{ cm}/\text{s}$. High-pressure H_2O vapor heat treatment achieved the passivation of thermally grown SiO_2/Si interfaces by reducing the recombination velocity. The sample with the as-deposited SiO_x layer on the top surface had a high recombination velocity, which markedly decreased from 1300 to $200 \text{ cm}/\text{s}$ as the light intensity increased from 0.315 to $3.27 \text{ mW}/\text{cm}^2$. It indicates that the as-deposited SiO_x/Si interface had substantial defect states that caused serious recombination of photo induced carriers. The recombination velocity was decreased by high-pressure H_2O vapor annealing to 60– $90 \text{ cm}/\text{s}$ similar to that of the sample coated with thermally grown SiO_2 layers. Figure 7 shows the calculated in depth distribution of photo-induced minority carrier density for illumination at $0.315 \text{ mW}/\text{cm}^2$. The photo

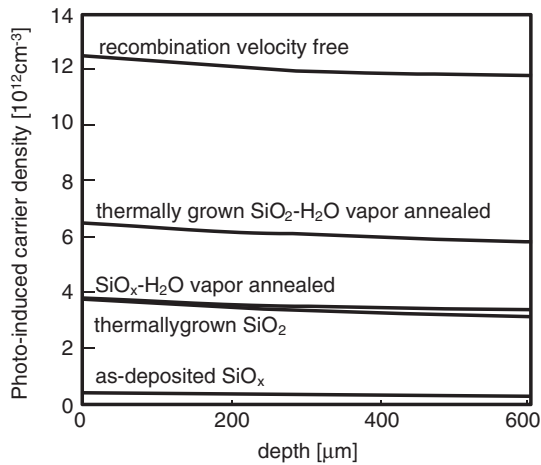


Fig. 7. Calculated in-depth distribution of photo induced carrier density for 532 nm light illumination at 0.315 mW/cm².

induced minority carrier density monotonically decreased from the top surface to the rear surface because of the photo induced carrier generation at the top surface caused by light illumination. It was the highest at $1.24 \times 10^{13} \text{ cm}^{-3}$ in the case of no recombination velocity and a minority carrier bulk lifetime of 1 ms. It was leveled off at the rear surface because of no recombination velocity. The peak photo induced minority carrier density decreased as the recombination velocity increased for the sample with both surfaces coated with thermally grown SiO₂ and the sample with the SiO_x layer deposited on the top surface and annealed with high-pressure H₂O vapor. It was very low at $3.9 \times 10^{11} \text{ cm}^{-3}$ because the recombination velocity was 1300 cm/s and there is serious carrier annihilation at the top surface for the sample with the as-deposited SiO_x layer on the top surface.

5. Conclusions

We reported free carrier absorption in order to analyze the electrical properties of silicon. A 9.35-GHz microwave interferometer was constructed using waveguide tubes having two narrow gaps for measurements of silicon wafers. We also developed a finite element numerical analysis program using theories of statistically thermodynamical semiconductor band, free carrier optical absorption, and the optical interference effect in order to calculate the microwave transmissivity. The transmissivity of 525-μm-thick silicon substrates that had different resistivities ranging from 4 to 1000 Ω cm were measured and also calculated. It decreased from 60.4 to 3.8% as the resistivity decreased from 1000 to 4 Ω cm. There was a good agreement between

measured and calculated results. Free carrier photo absorption caused by photo induced carriers was experimentally measured and numerically analyzed for 625 μm thick silicon samples coated with 100 nm thermally grown SiO₂ as well as SiO_x layers deposited on the top surface by the evaporation method. The 532 nm light illumination ranging from 0.315 to 3.27 mW/cm² decreased the transmissivity owing to free carrier absorption caused by photo induced free carriers. The present equipment detected photo induced minority carrier density per unit area of above $5 \times 10^{10} \text{ cm}^{-2}$. The effective minority carrier lifetime was analyzed. It increased from 360 to 540 cm/s for illumination at 0.315 mW/cm² by $1.3 \times 10^6 \text{ Pa}$ H₂O vapor heat treatment at 260 °C for 3 h in the case of thermally grown SiO₂/Si because of the passivation of SiO₂/Si interfaces. It markedly increased from 30 to 380 μs by the H₂O vapor heat treatment in the case of SiO_x layers deposited at the top surface. These were comparable to those measured using a conventional QSSPC equipment at 6.4 W/cm² light illumination. The recombination velocity was analyzed when the minority carrier bulk lifetime was assumed to be 1 ms. It was decreased from 78 to 30 cm/s for illumination at 0.315 mW/cm² by the $1.3 \times 10^6 \text{ Pa}$ H₂O vapor heat treatment at 260 °C for 3 h in the case of thermally grown SiO₂/Si because of the passivation of SiO₂/Si interfaces. It was markedly decreased from 1300 to 60 cm/s by the H₂O vapor heat treatment in the case of SiO_x layers deposited at the top surface.

Acknowledgments

The authors thank M. Kimura, Y. Sakakura, W. Kato, M. Saito, K. Morikawa, A. Mase, and A. Morimoto for their support.

- 1) K. Sakamoto and T. Sameshima: *Jpn. J. Appl. Phys.* **39** (2000) 2492.
- 2) M. J. Kerr and A. Cuevas: *Semicond. Sci. Technol.* **17** (2002) 166.
- 3) J. M. Borrego, R. J. Gutmann, N. Jensen, and O. Paz: *Solid-State Electron.* **30** (1987) 195.
- 4) G. S. Kousik, Z. G. Ling, and P. K. Ajmera: *J. Appl. Phys.* **72** (1992) 141.
- 5) T. Sameshima and M. Satoh: *Jpn. J. Appl. Phys.* **36** (1997) L687.
- 6) H. Engstrom: *J. Appl. Phys.* **51** (1980) 5245.
- 7) T. Sameshima, K. Saitoh, N. Aoyama, S. Higashi, M. Kondo, and A. Matsuda: *Jpn. J. Appl. Phys.* **38** (1999) 1892.
- 8) J. C. Irvin: *Bell Syst. Tech. J.* **41** (1962) 387.
- 9) K. Asada, K. Sakamoto, T. Watanabe, T. Sameshima, and S. Higashi: *Jpn. J. Appl. Phys.* **39** (2000) 3883.
- 10) M. Born and E. Wolf: *Principles of Optics* (Pergamon, New York, 1974) Chaps. 1 and 13.
- 11) A. S. Grove: *Physics and Technology of Semiconductor Devices* (Wiley, New York, 1967) Chap. 5.
- 12) A. G. Aberle, G. Heiser, and M. A. Green: *J. Appl. Phys.* **75** (1994) 5391.